



Published in final edited form as:

*Oncogene*. 2020 July ; 39(29): 5228–5239. doi:10.1038/s41388-020-1359-4.

## Mdm2 mediated neddylation of pVHL blocks the induction of anti-angiogenic factors.

Eric R. Wolf<sup>1</sup>, Alexander R. Mabry<sup>1</sup>, Blossom Damania<sup>2</sup>, Lindsey D. Mayo<sup>1,3,\*</sup>

<sup>1</sup>Department of Biochemistry & Molecular Biology, Indiana University School of Medicine, Indianapolis, IN 46202, USA

<sup>2</sup>Department of Microbiology and Immunology, University of North Carolina School of Medicine, Chapel Hill, NC, 27599, USA

<sup>3</sup>Department of Pediatrics, Indiana University School of Medicine, Indianapolis, IN 46202, USA

### Abstract

Mutations in the tumor suppressor *TP53* are rare in renal cell carcinomas. p53 is a key factor for inducing anti-angiogenic genes and RCC are highly vascularized, which suggests that p53 is inactive in these tumors. One regulator of p53 is the Mdm2 oncogene, which is correlated with high-grade, metastatic tumors. However, the sole activity of Mdm2 is not just to regulate p53, but it can also function independent of p53 to regulate the early stages of metastasis. Here, we report that the oncoprotein Mdm2 can bind directly to the tumor suppressor VHL, and conjugate nedd8 to VHL within a region that is important for the p53-VHL interaction. Nedd8 conjugated VHL is unable to bind to p53 thereby preventing the induction of anti-angiogenic factors. These results highlight a previously unknown oncogenic function of Mdm2 during the progression of cancer to promote angiogenesis through the regulation of VHL. Thus, the Mdm2-VHL interaction represents a pathway that impacts tumor angiogenesis.

### Keywords

angiogenesis; Mdm2; p53; thrombospondin; VHL

### Introduction

The murine double minute 2 (Mdm2) oncoprotein is detectable in 40–90% of human cancers and is correlated with high-grade metastatic tumors and poor patient outcomes [1]. The proposed canonical function of Mdm2 is its regulation of the tumor suppressor p53 through its activity as a ubiquitin E3 ligase [2, 3]. p53 plays a major role in the DNA damage response and cell cycle arrest by activating transcription of *CDKN1A*, *BAX*, *BBC3* and others [4–6]. p53 can also regulate transcription of genes involved in metabolism,

---

Users may view, print, copy, and download text and data-mine the content in such documents, for the purposes of academic research, subject always to the full Conditions of use:[http://www.nature.com/authors/editorial\\_policies/license.html#terms](http://www.nature.com/authors/editorial_policies/license.html#terms)

\*Correspondence: [ldmayo@iu.edu](mailto:ldmayo@iu.edu).

Competing Interests

The authors declare that they have no competing interests.

angiogenesis, stemness, migration, and invasion [reviewed in [7]]. As for angiogenesis, p53 can induce the transcription of several inhibitors such as *THSB1*, *SERPINE1*, and *COL18A1* and suppress transcription of the pro-angiogenic *VEGF* [8–12]. In this context, p53 would be considered a key repressor of angiogenesis. Blocking the anti-angiogenic activity of p53 is assumed to be regulated its antagonist Mdm2, via the ubiquitin ligase associated activity. Mdm2 is also associated with angiogenesis. In response to hypoxia, Mdm2 binds directly to hypoxia inducible factor 1 $\alpha$  (HIF1 $\alpha$ ) resulting in increased *VEGF* expression [13, 14]. Additionally, Mdm2 can bind to and stabilize the 3' UTR of *VEGF* mRNA [15]. Along with stabilizing HIF1 $\alpha$ , our lab recently showed that Mdm2 can be converted to a nedd8 E3 ligase in response to phosphorylation by c-Src. Mdm2 can then neddylate p53, rendering it stable but inactive which is a key event in response to growth factor stimulation [16].

In response to DNA damage, p53 can be activated by the von Hippel-Lindau tumor suppressor protein (VHL), which binds to p53 and blocks its Mdm2-mediated degradation [17]. VHL is commonly mutated in sporadic clear cell renal cell carcinomas and it plays an important role in hypoxic signaling through its regulation of HIF $\alpha$  subunits [18, 19]. Interestingly, p53 is rarely mutated in renal cell carcinomas, but p53 pathway genes are commonly downregulated suggesting a different mechanism of p53 pathway inhibition [20]. Interestingly, the region of VHL that binds to p53 contains a lysine that has been shown to be neddylated [21, 22], but its effect on binding to p53 was not examined [21].

Because VHL is able to stabilize and activate p53, and Mdm2 is able to disrupt p53 activity, we examined the impact of Mdm2 on VHL stabilization and activation of p53. Herein we show that the VHL-p53 interaction results in an increased production of inhibitors of angiogenesis and that Mdm2 is able to disrupt the binding of VHL to p53 through conjugation of nedd8 to VHL. To this end, we show that disruption of this pathway directly effects the secretion of thrombospondin-1 to promote angiogenesis. This study provides an explanation for the changes in p53 pathway genes seen in renal cell carcinomas as p53 activity is dependent on VHL.

## Results

### p53 target genes for apoptosis and angiogenesis are altered by VHL status

The tumor suppressor p53 is able to inhibit cancer progression via several different mechanisms, including the transcription of pro-apoptotic factors and anti-angiogenic factors [8, 10–12, 23]. Activation of p53 is a highly regulated process involving many other tumor suppressor proteins [24, 25]. It has been previously reported that in response to DNA damage VHL can bind to p53 and induce pro-apoptotic and cell cycle arrest genes *BAX* and *CDKN1A* [17]. We examined the TCGA using a subset of patient data for renal cell carcinomas, to determine the effects of mutations in the domain of VHL that binds to p53 on the mRNA levels of these target genes, as well as several other genes that p53 regulates. Interestingly, mutations in the  $\alpha$  domain of VHL caused an increase in mRNA for *BAX*, *CDKN1A*, and *BBC3* (Figure 1A). Likewise, the mRNA levels of the anti-angiogenic factors *THBS1*, *COL18A1*, and *SERPINE1* were also increased when the  $\alpha$  domain of VHL was mutated (Figure 1B). Importantly, mRNA levels of both VHL and p53 were not altered

between WT VHL and  $\alpha$  domain mutants of VHL (Figure 1C). *THBS1* codes for the protein thrombospondin-1 (TSP-1), a potent inhibitor of angiogenesis that is known to be regulated by p53 [8]. To confirm the importance of VHL on the transcription of *THBS1*, we analyzed the luciferase activity of a TSP-1 reporter in the 786-O and RCC4 cell lines with or without VHL transduction. In both cell lines, transduction with VHL increased the reporter activity by 3–4 fold (Figure 1D). In order to determine if the increase in *THBS1* transcription resulted in an increase in secreted TSP-1 protein, we analyzed conditioned media from 786-O and RCC4 cells for TSP-1 levels. Similar to the reporter activity results, VHL transduction increased the secreted TSP-1 protein levels by ~2 fold (Figure 1E). We also analyzed conditioned media using an angiogenesis microarray and saw consistent results (Figure S1A).

### **Mdm2 binds to VHL and inhibits VHL-p53 complex formation under hypoxia**

In order to determine the role for Mdm2 in the regulation of the VHL-p53 complex, we expressed exogenous Mdm2, VHL, and p53 in H1299 cells with or without hypoxia and analyzed complex formation by immunoprecipitation. The data in Figure 2A shows that VHL forms a complex with p53 under both normoxia and hypoxia, but this complex is prevented in the presence of Mdm2 under hypoxia. To examine if Mdm2 would form a complex with VHL in the absence of p53, we transiently expressed VHL and Mdm2 in p53 null H1299 cells. Immunoprecipitation of VHL was able to purify Mdm2 under both normoxia and hypoxia (Figure 2B). Endogenous Mdm2 and VHL also co-precipitated in extracts from MCF7 cells (Figure S2A). Since Mdm2 bound to VHL under both normoxia and hypoxia, but only inhibits VHL-p53 complex formation under hypoxia, we hypothesized that Mdm2 might be post-translationally modifying VHL under hypoxia. Of note, there is a neddylation site at lysine 159 of VHL that is contained within the region that binds p53 (Figure 2C) [21, 22]. Mdm2 functions as a neddylation E3 ligase under growth conditions [16], so we rationalized that Mdm2 could be neddylating VHL under certain signaling conditions. To further confirm the effect of Mdm2 on VHL-p53 complex formation, we transiently expressed VHL or VHL and Mdm2 in 786-O (null for VHL) cells and stained the cells with antibodies against VHL and p53 for immunofluorescence. Supporting the immunoprecipitation data, VHL colocalized with p53 under normoxia and Mdm2 inhibited this colocalization under hypoxia (Figure 2D and 2E).

### **Neddylation of VHL by Mdm2 interferes with VHL-p53 complex formation**

To determine if neddylation at K159 had an effect on VHL-p53 complex formation, we utilized a neddylation deficient mutant, K159E, of VHL. This mutant was isolated from a patient with Type 2C VHL disease, which only develops pheochromocytoma, as opposed to some more severe VHL disease mutants which can also cause kidney carcinomas [22, 26]. We transiently transfected H1299 cells with p53 and either WT VHL or K159E VHL under normoxia or hypoxia and analyzed VHL-p53 complex formation by immunoprecipitation (Figure 3A). VHL-p53 complex formation increased with the K159E mutant compared to WT, which was further increased under hypoxia. This data suggests that hypoxic conditions increase VHL neddylation. To determine if this increased complex formation was dependent on neddylation, we treated cells with MLN4924, a global neddylation inhibitor, and found that the VHL-p53 complex formation in 786-O (Figure 3B) and MCF7 (Figure 3C) cells was

increased. Additionally, treatment with PP1 resulted in increased VHL-p53 complex formation (Figure S2B). Since Mdm2 was shown to influence the VHL-p53 interaction, we tested if Mdm2 was the nedd8 E3 ligase for VHL. We first tested if Mdm2 binds directly to VHL using recombinant proteins produced and purified from bacteria. We found that Mdm2 bound to the  $\alpha$  domain of VHL (Figure 3D). Using an in vitro neddylation reaction with GST-VHL, His-Mdm2, and His-Src, Mdm2 neddylated VHL, and this activity was enhanced with Src (Figure 3E), as previously published [16]. In accordance with previously published data, the addition of MdmX to this reaction also increased the neddylation of VHL (Figure S2C) [27]. It has been shown that Src is phosphorylated at Y416 in response to hypoxia, and we verified this in our cells (Figure 3F) [28]. To determine if Mdm2 neddylated VHL in the cell, 786-O cells transduced with VHL or a control vector were transiently transfected with Mdm2 and endogenous nedd8 was immunoprecipitated from the cellular extracts. VHL was purified from cells with Mdm2 expressed, and this interaction increased under hypoxia (Figure 3G). Additionally, we transiently expressed components of our system with His-nedd8 and performed an Ni-NTA pulldown under denaturing conditions. Neddylation of VHL was evident with Mdm2 and constitutively active Src kinase, which was diminished with MLN4924 or using the K159E VHL mutant (Figure 3H).

### **VHL colocalizes with p53 under hypoxia or with treatment of MLN4924**

We analyzed colocalization using immunofluorescence confocal microscopy to determine if VHL-p53 complex formation was evident in the cell. 786-O cells were transiently transfected with WT VHL or K159E VHL and Mdm2 and stained with antibody against VHL and p53. We found that WT VHL colocalized with p53 when Mdm2 was not transfected or when Mdm2 was transfected with the addition of the neddylation inhibitor MLN4924 (Figure 4A). The K159E point mutant of VHL colocalized with p53 under all conditions tested in normal oxygen, including when Mdm2 was transfected (Figure 4B). Under hypoxic conditions, VHL only colocalized with p53 when cells were treated with MLN4924 (Figure 4C). There was an increase in colocalization of K159E VHL and p53 under hypoxia as compared to normoxia (Figure 4D). Transfection of Mdm2 with K159E VHL under hypoxia did not interfere with VHL-p53 colocalization. Interestingly, treatment with MLN4924 caused an additional increase in K159E VHL-p53 complex formation under hypoxia, suggesting that there may be additional neddylation sites that are important for this interaction (Figure 4D). To test this colocalization in an endogenous system, we treated Caki-1 cells with MLN4924 or DMSO (Control) under normoxia or hypoxia and stained with antibodies against VHL and p53. Similar to the results seen with the 786-O cell line, we found that p53 and VHL formed a complex under normoxia and hypoxia which was increased with MLN4924 treatment (Figure 4E and F). Of note the transient expression of VHL and p53 in cells showed phenotypic characteristics of cells undergoing apoptosis after 40 hrs. Caki-1 cells did not present this phenotype as they are exposed to MLN for shorter duration.

### **VHL activates p53 leading to increased transcription and secretion of TSP-1**

There are many signals that can activate p53-dependent transcription, but acetylation is necessary in order for p53 to actually bind to DNA [reviewed in [29]]. It has previously been shown that VHL activation of p53 results in acetylation at K373/382 of p53 in response to

DNA damage [17]. To determine if the activation of p53 under hypoxia would lead to increased transcription of *THBS1*, we examined the luciferase activity of a *THBS1* reporter gene in response to hypoxia with or without VHL. VHL reconstitution resulted in a significant increase in *THBS1* transcription, but this increase was negated by hypoxia (Figure 5A). Interestingly, treatment with MLN4924 overcame the hypoxia-dependent decrease in *THBS1* transcription (Figure 5A). To verify that the changes in *THBS1* transcription correlate with a change in protein secretion, we analyzed the protein levels of secreted TSP-1 by ELISA. Caki-1 cells were treated with MLN4924 and/or hypoxia and the secreted TSP-1 was measured. Hypoxia reduced the amount of TSP-1 secretion, and treatment with MLN4924 reversed this decrease (Figure 5B). VHL reconstitution increased the secretion of TSP-1 in both 786-O and RCC4 cells in normoxia (Figures 5C and D). Knockdown of p53 showed a marked decrease in TSP-1 secretion under hypoxia as compared to control cells with knockdown p53 (Figures 5C and 5D, S3A). Additionally, we examine if blocking the p53-Mdm2 interaction with Nutlin, a small molecule that binds the amino terminus of Mdm2 would change the induction of Thrombospondin. Nutlin treatment diminished Thrombospondin reporter activity (Figure S4A) in RCC4 VHL cells. Further analysis showed that p53 and Mdm2 proteins levels increased with Nutlin but pVHL remained unchanged (Figure S4B), and Nutlin prevented the binding of Mdm2 to p53 but did not have an effect on Mdm2-pVHL binding (Figure S4C). These data show that p53 and VHL are both required for a robust induction of TSP-1 in response to hypoxia and while Nutlin prevented the Mdm2-p53 interaction, the binding to pVHL was maintained.

### **p53 and TSP-1 inhibit Human Umbilical Vein Endothelial Cell network formation**

There are many factors that dictate whether or not angiogenesis will progress in a tumor. While it is evident that TSP-1 secretion is increased by VHL activation of p53, we wanted to gain a more holistic view of how this pathway affects angiogenesis. To this end, we transfected H1299 cells with p53 and either WT or K159R VHL and harvested conditioned media. We then cultured Human Umbilical Vein Endothelial Cells (HUVECs) in this conditioned media on growth factor reduced matrigel to monitor network formation as a readout for angiogenic potential. The addition of K159R VHL resulted in a significant decrease in network branch points compared to p53 alone (Figure 6A). The addition of an antibody against TSP-1 to the conditioned media, resulted in a significant increase in network branch points (angiogenesis) (Figure 6A). IgG isotype control had no effect on invitro tube formation (Figure S4D). Knocked down p53 in 786-O and RCC4 cells that had been previously transduced with VHL and harvested conditioned media under normoxia and hypoxia was used for angiogenesis assay. Conditioned media from 786-O cells with knockdown p53 caused a statistically significant increase in network branch points compared to both normoxia and a vector control under normoxia or hypoxia (Figure 6B). Similar to results seen using conditioned media from H1299 cells, the addition of IgG against TSP-1 caused an increase in branch point formation compared to control IgG (Figure S4D). Conditioned media from RCC4 cells induced angiogenesis in a similar pattern, with the exception that hypoxia alone was sufficient to cause an increase in branch point formation in the control cells (Figure 6C). Of note, 786-O cells are naturally null for HIF1 $\alpha$ , but maintain HIF2 $\alpha$ . RCC4 cells maintain both HIF1 $\alpha$  and HIF2 $\alpha$  expression, which may explain the more robust response to hypoxia in that cell line.

## Discussion

The regulation of angiogenesis in the context of neddylation has largely been defined in the regulation of migration of HUVECs and cancer associated fibroblast via Rho, and preventing apoptosis [30, 31]. This work suggest how the small molecule MLN 4924 may work in regulating the cells in the tumor microenvironment. We describe how an antiangiogenic pathway involving p53 and VHL can be disrupted by the neddylation activity of Mdm2. These data highlight an evolving understanding of both VHL and Mdm2 in the control of angiogenesis. The role of VHL in regulating angiogenesis through HIFs has been well studied and the mechanisms governing that interaction are well understood [18, 32–35]. The impact of Mdm2 on angiogenesis has been previously described, but there is a gap in our understanding of the mechanisms Mdm2 uses to promote angiogenesis. Mdm2 can regulate angiogenesis independent of HIF1 $\alpha$  and *VEGF* stabilization, and these functions of Mdm2 are still being explored [36–39].

Recent work in our lab suggests that Mdm2 is a driving force for early stage metastasis, which implicates Mdm2 in the vascularization of tumors [40]. We have also recently shown that Mdm2 is converted to a neddylation enzyme in response to phosphorylation by the kinase c-Src. In response to various growth conditions c-Src phosphorylates Mdm2, which in turn neddylates p53 to render it stable but inactive [16]. It is likely that the neddylation of p53 functions in tandem with the neddylation of VHL in order to completely shut down the transcriptional activity of p53. Likewise, the effect of MLN4924 treatment probably alleviates repression of both p53 and VHL and allows them to continue their tumor suppressive function. c-Src governs many tumorigenic pathways, including angiogenesis, and is activated in response to hypoxic conditions [28, 41]. This led us to examine the effect of the c-Src/Mdm2 pathway on angiogenesis inhibition regulated by p53. Mdm2 has been shown to block the transcriptional activity of p53 independent of its ubiquitination and neddylation functions in an indirect manner, so we investigated activators of p53 as potential targets of Mdm2.

In addition to its regulation of p53, Mdm2 has many other interactions that impact various activators of p53 in order to indirectly impact p53 function [42–47]. The role of p53 in hypoxia has been studied, but there are conflicting reports. There are issues with interpreting the data due to variations in what different groups define as hypoxia (i.e., 0.01% O<sub>2</sub> vs 10% O<sub>2</sub>), but the consensus is that HIF1 $\alpha$  binds to p53 [43, 48–54]. Due to the intricate web of feedback loops and interactions surrounding the p53/Mdm2/HIF/VHL signaling axes, it has been previously suggested that there is some interaction between VHL and Mdm2 that would be important for cancer signaling [17].

In addition to the previously reported genes involved in cell cycle arrest and apoptosis, we show in a subset of patients with clear cell renal cell carcinoma that VHL is important for the activation of p53 for several genes involved in angiogenesis (Figure 1). It is unclear at the moment if different VHL disease types will have different levels of p53 activation. However, the K159E VHL mutant used in this study was isolated from a patient with a Type 2C VHL disease mutation [22]. Importantly, this category of VHL disease does not develop kidney neoplasms [26]. The mutations for different VHL disease types are categorized based



on the clinical presentation of the disease as opposed to the location of the mutation on the gene [55]. It will be interesting to see in the future how different VHL disease mutants respond to this signaling pathway. Interestingly, every VHL disease mutant that has been tested has a defect in binding to fibronectin, and neddylation of VHL has been suggested to regulate fibronectin matrix assembly [22]. It is possible that some mutations of VHL may actually protect against kidney cancer by changing the binding activity of the protein.

p53 is rarely mutated in renal cell carcinoma, but many target genes of p53 are downregulated in these tumors [20]. For many years, there were conflicting reports on the effect of p53 upregulation and subsequent Mdm2 upregulation in renal cell carcinomas. However, a consensus has recently emerged that shows a correlation between p53 upregulation and disease progression [reviewed in [56]]. This suggests that there are other pathways involved in shutting down the p53 signaling axis. Our data support a role for VHL as a likely source of this dysregulation as it is highly mutated in renal cell carcinoma and is an activator of p53 [17]. But this does not explain the incidence of tumors that maintain both wild type p53 and wild type VHL. A possible explanation is the role of Mdm2 in the development of renal cell carcinoma as patients with high protein expression of both p53 and Mdm2 have the poorest overall survival [57]. This data, combined with our study, highlights the importance of Mdm2 signaling in renal cell carcinoma. We have presented one mechanism that Mdm2 uses to disrupt normal p53 signaling to promote angiogenesis and tumor progression. Additionally, Mdm2 neddylation of p53 increases the stability of p53 but makes it inactive [16]. This could be part of the reason why high levels of wild type p53 are associated with poor outcomes in ccRCC. It is likely that there are other mechanisms to ensure redundancy in the function of Mdm2, and these pathways are currently being explored. This study provides the impetus for Mdm2 to be considered as a prognostic marker and potential therapeutic target in renal cell carcinomas.

## Materials and Methods

### Cell culture

All human cell lines (786-O, RCC4, H1299, MCF7, and BJ) were cultured in DMEM with 8% FBS supplemented with penicillin and streptomycin at 37° C in a humidified incubator in 5% CO<sub>2</sub>. Cell lines were maintained according to ATCC guidelines. For hypoxia experiments, cells were cultured in DMEM/F12 1:1 and placed at 37° C in a humidified incubator with 1% O<sub>2</sub>.

### Protein purification

Recombinant proteins (GST, GST-alpha VHL, GST-beta VHL, GST-VHL, His-Mdm2, and GST-p300 HAT domain) were produced in BL21DE3 cells and purified as previously described [58, 59]. His-Src was purchased from Millipore and the neddylation reaction components were purchased from Boston Biochem.

### Thrombospondin-1 Reporter Assay

H1299, 786-O, RCC4, or Caki-1 cells were transfected with a reporter construct for thrombospondin-1 as previously described [16]. Luciferase activity was measured following transfection for 40 hours, with 16 hours of MLN4924 when noted in the figures.

### Secreted Thrombospondin-1

786-O and RCC4 cells were cultured in DMEM for 48 hours. Media was harvested and passed through a nitrocellulose membrane using a Bio-Dot microfiltration apparatus (BioRad). The membrane was then incubated with an antibody for TSP-1 (A6.1, Santa Cruz) and analyzed by Western blot. Resulting images were quantified using the Dot Blot Analyzer plugin for ImageJ.

### Enzyme-linked Immunosorbent Assay

H1299 cells were transfected according to figure labels using polyethylenimine for 24 hours, followed by 21% or 1% O<sub>2</sub> culturing for 24 hours. 786-O and RCC4 cells were cultured in 21% or 1% O<sub>2</sub> for 24 hours. All media was harvested and analyzed using an ELISA kit for TSP-1 (Ray Biotech) with a 10% dilution of conditioned media.

### Immunoprecipitation

Following transfection and/or treatment as described, cells were lysed in lysis buffer with protease inhibitor and 20 mM N-ethylmaleimide and incubated for 2 hours at 4° C with Protein-G agarose beads which had been pre-incubated with antibody. Following incubation, beads were washed 3x with lysis buffer for 10 minutes at 4° C. After the final wash, 6X Lamelli dye was added to the beads and samples were boiled for 10 minutes at 100° C and separated by SDS-PAGE.

### Western blot

Whole cell lysates, immunoprecipitated proteins, pulldown assays, and in vitro reactions were all subjected to SDS-PAGE and transferred to PVDF membrane. Western blots for HA (12CA5, Roche), p53 (DO-1, Santa Cruz), Mdm2 (2A10, 2A9, 4B2), VHL (VHL40, FL-181, Santa Cruz), GST (B-14, Santa Cruz), HIF1 $\alpha$  (H1 $\alpha$ 67, Santa Cruz), Ac-p53 K373/382 (Upstate Signaling), GAPDH (6C5, Santa Cruz), and NEDD8 (A-812, Boston Biochem) were performed according to the manufacturers' protocols.

### Immunofluorescence microscopy

786-O, RCC4, or Caki-1 cells were grown on glass coverslips and transfected with WT or K159E VHL and Mdm2. Following transfection for 24 hours, cells were treated with MLN4924 or a control for an additional 16 hours. Cells were fixed in 4% paraformaldehyde in PBS for 15 minutes, washed with PBS, and permeabilized in 1% Triton X-100 in PBS for 15 minutes. Coverslips were blocked in 5% bovine serum albumin for 1 hour in PBS/Tween before being stained with p53 and VHL antibodies. Coverslips were mounted to slides using ProLong Diamond Antifade Mountant with DAPI (Life Technologies). Slides were visualized on a Leica SP8 MP microscope.



### Tube forming assay

H1299 cells were transfected according to the figure panels for 48 hours followed by media harvest. 786-O and RCC4 cells were cultured in 21% or 1% O<sub>2</sub> for 48 hours followed by media harvest. Growth factor reduced matrigel (Corning) was plated in a 96-well plate and allowed to set according to the manufacturer's guidelines. GFP<sup>+</sup> Human Umbilical Vein Endothelial Cells were plated on top of the matrigel in 10% EBM-2/EGM-2 (Lonza) and 90% conditioned media.

### Bioinformatics analysis of clinical data

Data was analyzed from KIRC\_TCGA\_PUB downloaded from [cbioportal.org](http://cbioportal.org). Only samples with wild type p53 were included. 62 samples with alpha domain mutations in VHL were included and 72 samples with wild type VHL were included.

### His-nedd8 Pulldown

H1299 cells were transfected with His-nedd8 and other plasmids as shown in the figure panels. 24 hours after transfection, cells were treated with MLN4924 or a control for an additional 16 hours. Cells were lysed in denaturing conditions (6 M guanidinium-HCl, 0.1 M Na<sub>2</sub>HPO<sub>4</sub>/NaH<sub>2</sub>PO<sub>4</sub>, 0.01 M Tris-HCl, pH 8.0, 5 mM imidazole, and 10 mM β-mercaptoethanol) and sonicated. Lysates were incubated with 30 μL Ni<sup>2+</sup>-NTA beads (Qiagen) for 2 hours at 4° C with rotation. The beads were washed and eluted as previously described and subjected to SDS-PAGE [16].

### In vitro neddylation assays

GST-VHL (500ng) was incubated with 1 μg of His-Mdm2, 30 μM nedd8 (Boston Biochem), 200 nM E1 (APPBP1/UBA3, Boston Biochem), 0.5 μM E2 (UbcH12, Boston Biochem), and 1.25 mM ATP in nedd8 reaction buffer (50 mM Tris, 150 mM NaCl, 2.5 mM MgCl<sub>2</sub>, pH 7.6) at 37° C for one hour followed by SDS-PAGE.

### Quantification and statistical analysis

All data were analyzed and statistics calculated using GraphPad Prism 8. Biological replicates were conducted for each experiment and the data was repeated at least three times.

### Supplementary Material

Refer to Web version on PubMed Central for supplementary material.

### Acknowledgments

This research was supported by NIH/NCI CA172256 and the Riley Children's Foundation. We thank Dr. Ohh for the VHL expression plasmid, Dr. Bouck for the Thrombospondin reporter plasmid, and Dr. Ivan for the renal cell carcinoma cell lines to aid in this study.

### References

1. Rayburn E, Zhang R, He J, Wang H. MDM2 and human malignancies: expression, clinical pathology, prognostic markers, and implications for chemotherapy. *Curr Cancer Drug Targets* 2005; 5: 27–41. [PubMed: 15720187]

2. Haupt Y, Maya R, Kazaz A, Oren M. Mdm2 promotes the rapid degradation of p53. *Nature* 1997; 387: 296–299. [PubMed: 9153395]
3. Kubbutat MH, Jones SN, Vousden KH. Regulation of p53 stability by Mdm2. *Nature* 1997; 387: 299–303. [PubMed: 9153396]
4. Miyashita T, Reed JC. Tumor suppressor p53 is a direct transcriptional activator of the human bax gene. *Cell* 1995; 80: 293–299. [PubMed: 7834749]
5. el-Deiry WS, Tokino T, Velculescu VE, Levy DB, Parsons R, Trent JM et al. WAF1, a potential mediator of p53 tumor suppression. *Cell* 1993; 75: 817–825. [PubMed: 8242752]
6. Han J, Flemington C, Houghton AB, Gu Z, Zambetti GP, Lutz RJ et al. Expression of bbc3, a proapoptotic BH3-only gene, is regulated by diverse cell death and survival signals. *Proc Natl Acad Sci U S A* 2001; 98: 11318–11323. [PubMed: 11572983]
7. Joerger AC, Fersht AR. The p53 Pathway: Origins, Inactivation in Cancer, and Emerging Therapeutic Approaches. *Annu Rev Biochem* 2016; 85: 375–404. [PubMed: 27145840]
8. Dameron KM, Volpert OV, Tainsky MA, Bouck N. Control of angiogenesis in fibroblasts by p53 regulation of thrombospondin-1. *Science* 1994; 265: 1582–1584. [PubMed: 7521539]
9. Kamat CD, Green DE, Warnke L, Thorpe JE, Ceriello A, Ihnat MA. Mutant p53 facilitates proangiogenic, hyperproliferative phenotype in response to chronic relative hypoxia. *Cancer Lett* 2007; 249: 209–219. [PubMed: 16997458]
10. Zou Z, Gao C, Nagaich AK, Connell T, Saito S, Moul JW et al. p53 regulates the expression of the tumor suppressor gene maspin. *J Biol Chem* 2000; 275: 6051–6054. [PubMed: 10692390]
11. Miled C, Pontoglio M, Garbay S, Yaniv M, Weitzman JB. A genomic map of p53 binding sites identifies novel p53 targets involved in an apoptotic network. *Cancer Res* 2005; 65: 5096–5104. [PubMed: 15958553]
12. Mukhopadhyay D, Tsiokas L, Sukhatme VP. Wild-type p53 and v-Src exert opposing influences on human vascular endothelial growth factor gene expression. *Cancer Res* 1995; 55: 6161–6165. [PubMed: 8521408]
13. Joshi S, Singh AR, Durden DL. MDM2 regulates hypoxic hypoxia-inducible factor 1alpha stability in an E3 ligase, proteasome, and PTEN-phosphatidylinositol 3-kinase-AKT-dependent manner. *J Biol Chem* 2014; 289: 22785–22797. [PubMed: 24982421]
14. Nieminen AL, Qanungo S, Schneider EA, Jiang BH, Agani FH. Mdm2 and HIF-1alpha interaction in tumor cells during hypoxia. *J Cell Physiol* 2005; 204: 364–369. [PubMed: 15880652]
15. Zhou S, Gu L, He J, Zhang H, Zhou M. MDM2 regulates vascular endothelial growth factor mRNA stabilization in hypoxia. *Mol Cell Biol* 2011; 31: 4928–4937. [PubMed: 21986500]
16. Batuello CN, Hauck PM, Gendron JM, Lehman JA, Mayo LD. Src phosphorylation converts Mdm2 from a ubiquitinating to a neddylation E3 ligase. *Proc Natl Acad Sci U S A* 2015; 112: 1749–1754. [PubMed: 25624478]
17. Roe JS, Kim H, Lee SM, Kim ST, Cho EJ, Youn HD. p53 stabilization and transactivation by a von Hippel-Lindau protein. *Mol Cell* 2006; 22: 395–405. [PubMed: 16678111]
18. Ivan M, Kondo K, Yang H, Kim W, Valiando J, Ohh M et al. HIF1alpha targeted for VHL-mediated destruction by proline hydroxylation: implications for O2 sensing. *Science* 2001; 292: 464–468. [PubMed: 11292862]
19. Kim WY, Kaelin WG. Role of VHL gene mutation in human cancer. *J Clin Oncol* 2004; 22: 4991–5004. [PubMed: 15611513]
20. Gurova KV, Hill JE, Razorenova OV, Chumakov PM, Gudkov AV. p53 pathway in renal cell carcinoma is repressed by a dominant mechanism. *Cancer Res* 2004; 64: 1951–1958. [PubMed: 15026329]
21. Russell RC, Ohh M. NEDD8 acts as a ‘molecular switch’ defining the functional selectivity of VHL. *EMBO Rep* 2008; 9: 486–491. [PubMed: 18323857]
22. Stickle NH, Chung J, Klco JM, Hill RP, Kaelin WG Jr., Ohh M. pVHL modification by NEDD8 is required for fibronectin matrix assembly and suppression of tumor development. *Mol Cell Biol* 2004; 24: 3251–3261. [PubMed: 15060148]
23. Nishimori H, Shiratsuchi T, Urano T, Kimura Y, Kiyono K, Tatsumi K et al. A novel brain-specific p53-target gene, BAI1, containing thrombospondin type 1 repeats inhibits experimental angiogenesis. *Oncogene* 1997; 15: 2145–2150. [PubMed: 9393972]

24. Wolf ER, McAtarsney CP, Bredhold KE, Kline AM, Mayo LD. Mutant and wild-type p53 form complexes with p73 upon phosphorylation by the kinase JNK. *Sci Signal* 2018; 11.
25. Somasundaram K, MacLachlan TK, Burns TF, Sgagias M, Cowan KH, Weber BL et al. BRCA1 signals ARF-dependent stabilization and coactivation of p53. *Oncogene* 1999; 18: 6605–6614. [PubMed: 10597265]
26. Zbar B, Kishida T, Chen F, Schmidt L, Maher ER, Richards FM et al. Germline mutations in the Von Hippel-Lindau disease (VHL) gene in families from North America, Europe, and Japan. *Hum Mutat* 1996; 8: 348–357. [PubMed: 8956040]
27. Hauck PM, Wolf ER, Olivos DJ 3rd, McAtarsney CP, Mayo LD. The fate of murine double minute X (MdmX) is dictated by distinct signaling pathways through murine double minute 2 (Mdm2). *Oncotarget* 2017; 8: 104455–104466. [PubMed: 29262653]
28. Mukhopadhyay D, Tsiokas L, Zhou XM, Foster D, Brugge JS, Sukhatme VP. Hypoxic induction of human vascular endothelial growth factor expression through c-Src activation. *Nature* 1995; 375: 577–581. [PubMed: 7540725]
29. Reed SM, Quelle DE. p53 Acetylation: Regulation and Consequences. *Cancers (Basel)* 2014; 7: 30–69. [PubMed: 25545885]
30. Jin Y, Zhang P, Wang Y, Jin B, Zhou J, Zhang J et al. Neddylation Blockade Diminishes Hepatic Metastasis by Dampening Cancer Stem-Like Cells and Angiogenesis in Uveal Melanoma. *Clin Cancer Res* 2018; 24: 3741–3754. [PubMed: 29233905]
31. Yao WT, Wu JF, Yu GY, Wang R, Wang K, Li LH et al. Suppression of tumor angiogenesis by targeting the protein neddylation pathway. *Cell Death Dis* 2014; 5: e1059. [PubMed: 24525735]
32. Jaakkola P, Mole DR, Tian YM, Wilson MI, Gielbert J, Gaskell SJ et al. Targeting of HIF- $\alpha$  to the von Hippel-Lindau ubiquitylation complex by O<sub>2</sub>-regulated prolyl hydroxylation. *Science* 2001; 292: 468–472. [PubMed: 11292861]
33. Lonergan KM, Iliopoulos O, Ohh M, Kamura T, Conaway RC, Conaway JW et al. Regulation of hypoxia-inducible mRNAs by the von Hippel-Lindau tumor suppressor protein requires binding to complexes containing elongins B/C and Cul2. *Mol Cell Biol* 1998; 18: 732–741. [PubMed: 9447969]
34. Ohh M, Park CW, Ivan M, Hoffman MA, Kim TY, Huang LE et al. Ubiquitination of hypoxia-inducible factor requires direct binding to the beta-domain of the von Hippel-Lindau protein. *Nat Cell Biol* 2000; 2: 423–427. [PubMed: 10878807]
35. Stebbins CE, Kaelin WG Jr., Pavletich NP. Structure of the VHL-ElonginC-ElonginB complex: implications for VHL tumor suppressor function. *Science* 1999; 284: 455–461. [PubMed: 10205047]
36. Venkatesan T, Alaseem A, Chinnaiyan A, Dhandayuthapani S, Kanagasabai T, Alhazzani K et al. MDM2 Overexpression Modulates the Angiogenesis-Related Gene Expression Profile of Prostate Cancer Cells. *Cells* 2018; 7.
37. Xiong J, Yang Q, Li J, Zhou S. Effects of MDM2 inhibitors on vascular endothelial growth factor-mediated tumor angiogenesis in human breast cancer. *Angiogenesis* 2014; 17: 37–50. [PubMed: 23907365]
38. Patterson DM, Gao D, Trahan DN, Johnson BA, Ludwig A, Barbieri E et al. Effect of MDM2 and vascular endothelial growth factor inhibition on tumor angiogenesis and metastasis in neuroblastoma. *Angiogenesis* 2011; 14: 255–266. [PubMed: 21484514]
39. Ding X, Jia X, Wang C, Xu J, Gao SJ, Lu C. A DHX9-lncRNA-MDM2 interaction regulates cell invasion and angiogenesis of cervical cancer. *Cell Death Differ* 2018.
40. Hauck PM, Wolf ER, Olivos DJ 3rd, Batuello CN, McElyea KC, McAtarsney CP et al. Early-Stage Metastasis Requires Mdm2 and Not p53 Gain of Function. *Mol Cancer Res* 2017; 15: 1598–1607. [PubMed: 28784612]
41. Eliceiri BP, Paul R, Schwartzberg PL, Hood JD, Leng J, Cheresch DA. Selective requirement for Src kinases during VEGF-induced angiogenesis and vascular permeability. *Mol Cell* 1999; 4: 915–924. [PubMed: 10635317]
42. Bohlman S, Manfredi JJ. p53-independent effects of Mdm2. *Subcell Biochem* 2014; 85: 235–246. [PubMed: 25201198]

43. Chen D, Li M, Luo J, Gu W. Direct interactions between HIF-1 alpha and Mdm2 modulate p53 function. *J Biol Chem* 2003; 278: 13595–13598. [PubMed: 12606552]
44. Ganguli G, Wasylyk B. p53-independent functions of MDM2. *Mol Cancer Res* 2003; 1: 1027–1035. [PubMed: 14707286]
45. Zeng X, Chen L, Jost CA, Maya R, Keller D, Wang X et al. MDM2 suppresses p73 function without promoting p73 degradation. *Mol Cell Biol* 1999; 19: 3257–3266. [PubMed: 10207051]
46. Wang XQ, Ongkeko WM, Lau AW, Leung KM, Poon RY. A possible role of p73 on the modulation of p53 level through MDM2. *Cancer Res* 2001; 61: 1598–1603. [PubMed: 11245471]
47. Kadakia M, Slader C, Berberich SJ. Regulation of p63 function by Mdm2 and MdmX. *DNA Cell Biol* 2001; 20: 321–330. [PubMed: 11445003]
48. An WG, Kanekal M, Simon MC, Maltepe E, Blagosklonny MV, Neckers LM. Stabilization of wild-type p53 by hypoxia-inducible factor 1alpha. *Nature* 1998; 392: 405–408. [PubMed: 9537326]
49. Graeber TG, Peterson JF, Tsai M, Monica K, Fornace AJ Jr., Giaccia AJ. Hypoxia induces accumulation of p53 protein, but activation of a G1-phase checkpoint by low-oxygen conditions is independent of p53 status. *Mol Cell Biol* 1994; 14: 6264–6277. [PubMed: 8065358]
50. Hammond EM, Denko NC, Dorie MJ, Abraham RT, Giaccia AJ. Hypoxia links ATR and p53 through replication arrest. *Mol Cell Biol* 2002; 22: 1834–1843. [PubMed: 11865061]
51. Hansson LO, Friedler A, Freund S, Rudiger S, Fersht AR. Two sequence motifs from HIF-1alpha bind to the DNA-binding site of p53. *Proc Natl Acad Sci U S A* 2002; 99: 10305–10309. [PubMed: 12124396]
52. Mizuno S, Bogaard HJ, Kraskauskas D, Alhussaini A, Gomez-Arroyo J, Voelkel NF et al. p53 Gene deficiency promotes hypoxia-induced pulmonary hypertension and vascular remodeling in mice. *Am J Physiol Lung Cell Mol Physiol* 2011; 300: L753–761. [PubMed: 21335523]
53. Pan Y, Oprysko PR, Asham AM, Koch CJ, Simon MC. p53 cannot be induced by hypoxia alone but responds to the hypoxic microenvironment. *Oncogene* 2004; 23: 4975–4983. [PubMed: 15107830]
54. Sanchez-Puig N, Veprintsev DB, Fersht AR. Binding of natively unfolded HIF-1alpha ODD domain to p53. *Mol Cell* 2005; 17: 11–21. [PubMed: 15629713]
55. Kaelin WG. Von Hippel-Lindau disease. *Annu Rev Pathol* 2007; 2: 145–173. [PubMed: 18039096]
56. Noon AP, Vlatkovic N, Polanski R, Maguire M, Shawki H, Parsons K et al. p53 and MDM2 in renal cell carcinoma: biomarkers for disease progression and future therapeutic targets? *Cancer* 2010; 116: 780–790. [PubMed: 20052733]
57. Haitel A, Wiener HG, Baethge U, Marberger M, Susani M. mdm2 expression as a prognostic indicator in clear cell renal cell carcinoma: comparison with p53 overexpression and clinicopathological parameters. *Clin Cancer Res* 2000; 6: 1840–1844. [PubMed: 10815906]
58. Li AG, Piluso LG, Cai X, Wei G, Sellers WR, Liu X. Mechanistic insights into maintenance of high p53 acetylation by PTEN. *Mol Cell* 2006; 23: 575–587. [PubMed: 16916644]
59. Wu X, Bayle JH, Olson D, Levine AJ. The p53-mdm-2 autoregulatory feedback loop. *Genes Dev* 1993; 7: 1126–1132. [PubMed: 8319905]

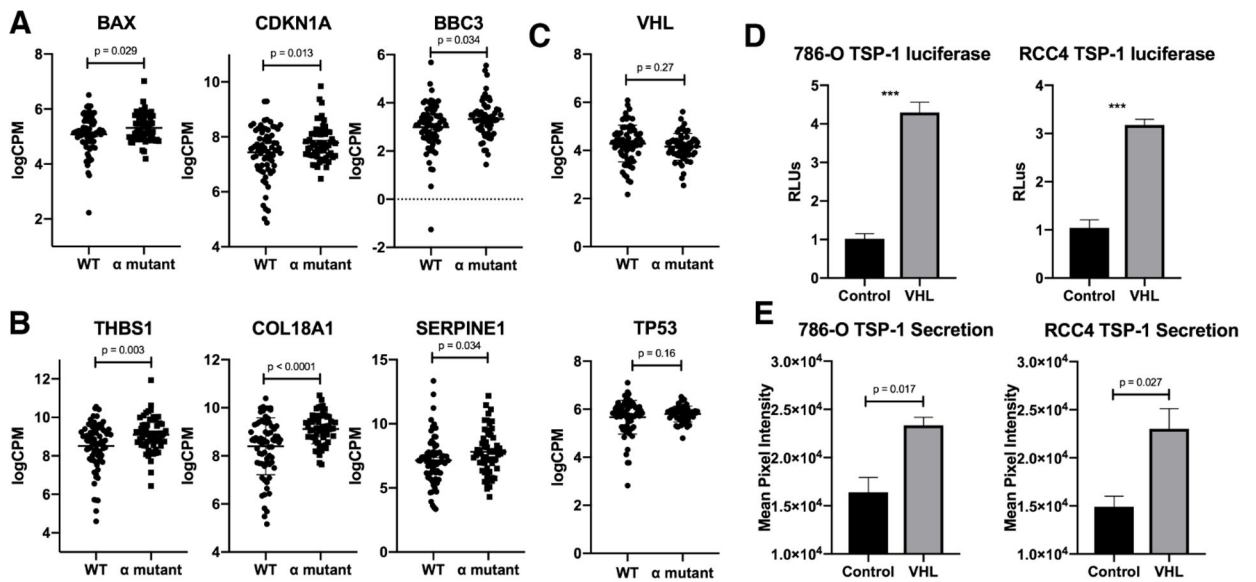


**Figure 1. p53 target genes for apoptosis and angiogenesis are altered by VHL status** (A-B) Log counts per million for *BAX*, *CDKN1A*, and *BBC3* (A) or *THBS1*, *COL18A1*, and *SERPINE1* (B). Only samples with wild-type p53 were included in the analysis. WT refers to wild type VHL status, and  $\alpha$  mutant refers to any point mutation within the  $\alpha$  domain of VHL. Error bars represent SEM. P values were calculated using an unpaired t test.

(C) Luciferase assay in 786-O and RCC4 cells with or without VHL for thrombospondin-1 plotted as relative luciferase units. Means are calculated from three biological replicates. Error bars represent SEM. Statistics were calculated using an unpaired t test (\*\* $p < 0.001$ ).

(D) Dot blot assay to measure protein level of thrombospondin-1 in media secreted from 786-O or RCC4 cells with or without VHL. Means are calculated from three biological replicates. Error bars represent SEM. Statistics were calculated using an unpaired t test (\*\* $p < 0.001$ ).

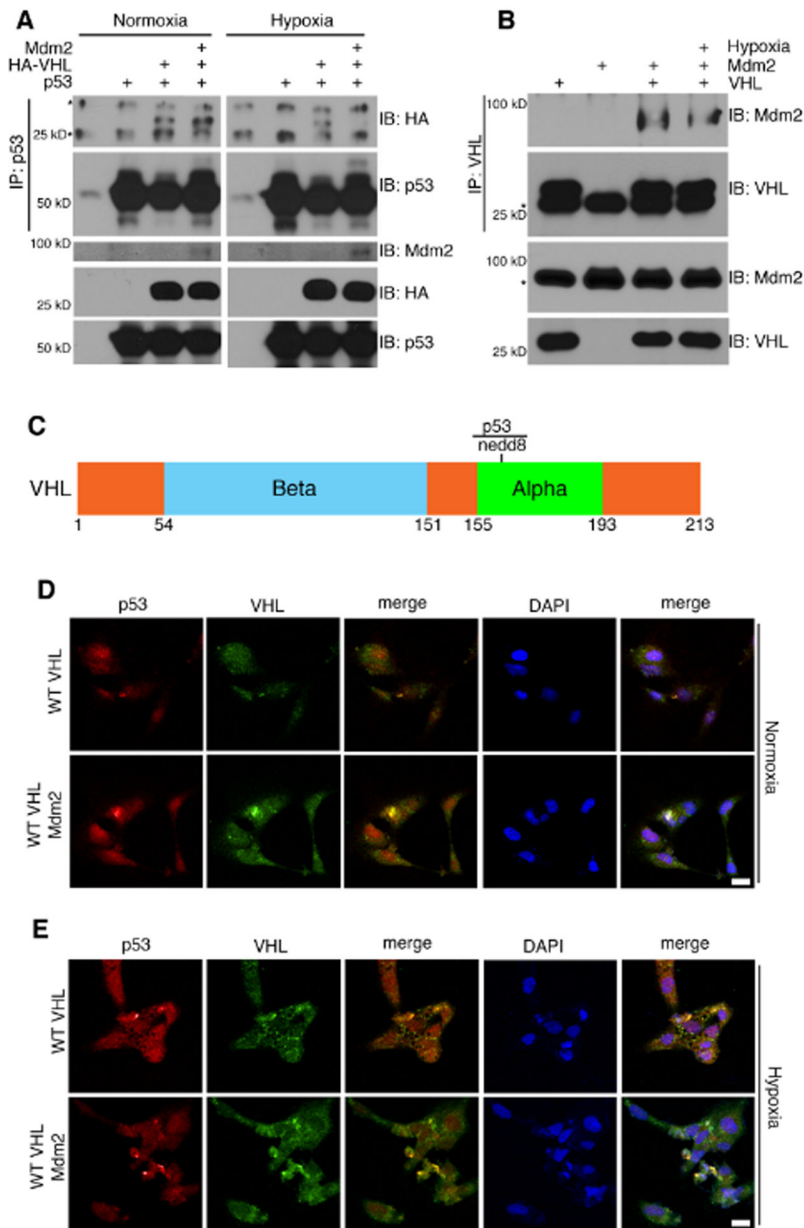


**Figure 2. Mdm2 binds to VHL and inhibits VHL-p53 complex formation under hypoxia**  
 (A-B) Transient transfection in H1299 cells followed by incubation in either normoxia or hypoxia. p53 (A) or VHL (B) was immunoprecipitated from cell lysates and subjected to analysis by Western blot.  
 (C) Schematic of VHL protein showing the primary site of neddylation, as well as the region that has been shown to be indispensable for binding to p53.  
 (D-E) Transfection of 786-O cells with VHL or VHL and Mdm2 under normoxia (D) or hypoxia (E). Cells were fixed and stained with antibody against p53 and VHL and subjected to immunofluorescence confocal microscopy. Scale bar represents 25  $\mu$ m.



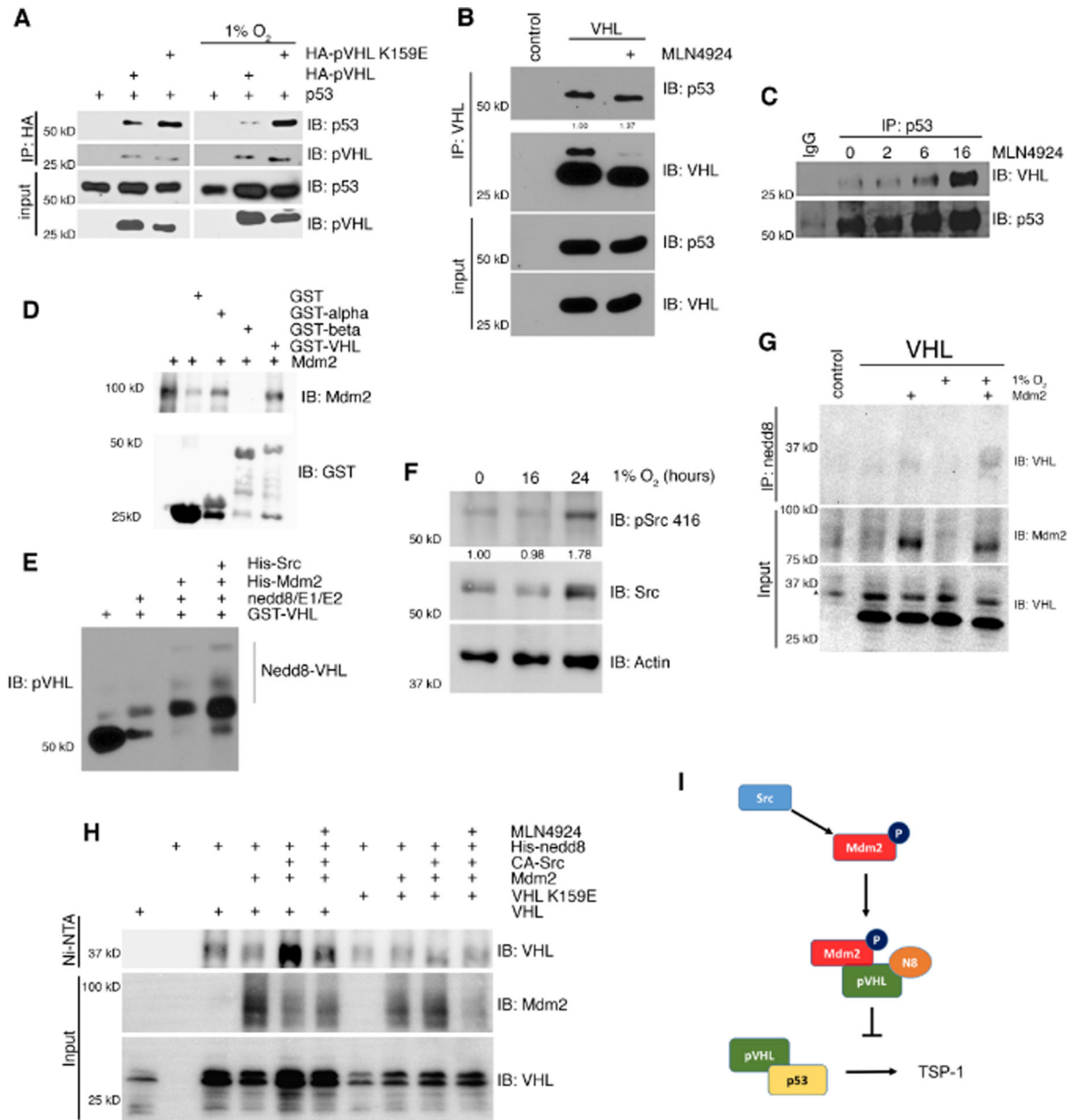


**Figure 3. Nedd8ylation of VHL by Mdm2 interferes with VHL-p53 complex formation**

(A) Transient transfection in H1299 cells under normoxia or hypoxia. Cell lysates were immunoprecipitated for HA and subjected to analysis by Western blot.

(B) Immunoprecipitation of VHL from 786-O cells treated with the neddylation inhibitor MLN4924 and Western blotted for p53 and VHL.

(C) Immunoprecipitation of p53 or IgG control from MCF7 cells treated with MLN4924 for various indicated times and Western blotted for VHL and p53.

(D) GST pull-down of GST, GST-alpha VHL, GST-beta VHL, or GST-VHL with His-Mdm2 and Western blotted for GST and Mdm2.

(E) Cell free neddylation assay using recombinant proteins. Reactions were separated by SDS-PAGE and analyzed by Western blot.

(F) Immunoprecipitation of endogenous nedd8 from 786-O cells transfected with Mdm2 and subjected to hypoxia and Western blotted for VHL and Mdm2.

(G) Ni-NTA pulldown for His-nedd8 in H1299 cells in a transient transfection and subjected to treatment with MLN4924. Samples were separated with SDS-PAGE and analyzed by Western blot for VHL and Mdm2.

(H) Schematic of the p53-pVHL-Thrombospondin pathway disrupted by c-Src-Mdm2.

Author Manuscript

Author Manuscript

Author Manuscript

Author Manuscript

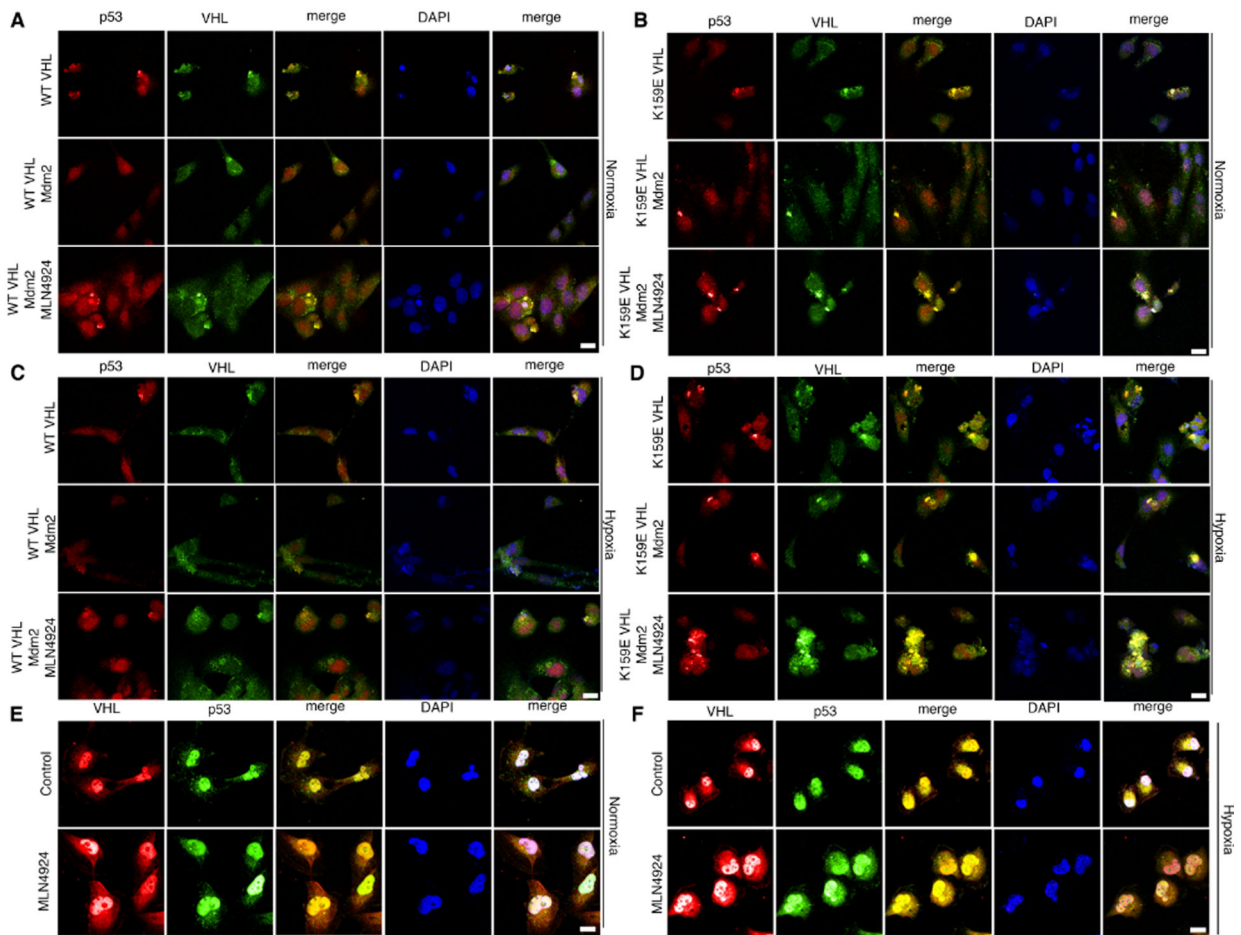


**Figure 4. VHL forms a complex with p53 under hypoxia or with treatment of MLN4924**  
 (A-B) Transfection of 786-O cells with WT VHL (A) or K159E VHL (B) and Mdm2 under normoxia. Cells were treated with MLN4924 or a control, fixed, and stained with antibodies against p53 and VHL and subjected to immunofluorescence confocal microscopy. Scale bar represents 25  $\mu$ m.  
 (C-D) Transfection of 786-O cells with WT VHL (C) or K159E (D) VHL and Mdm2 under hypoxia. Cells were treated with MLN4924 or a control, fixed, and stained with antibodies against p53 and VHL and subjected to immunofluorescence confocal microscopy. Scale bar represents 25  $\mu$ m.  
 (E-F) Immunofluorescence microscopy of Caki-1 cells treated with MLN4924 or a control under normoxia (E) or hypoxia (F). Cells were fixed and stained with antibodies against VHL and p53. Scale bar represents 50  $\mu$ m.

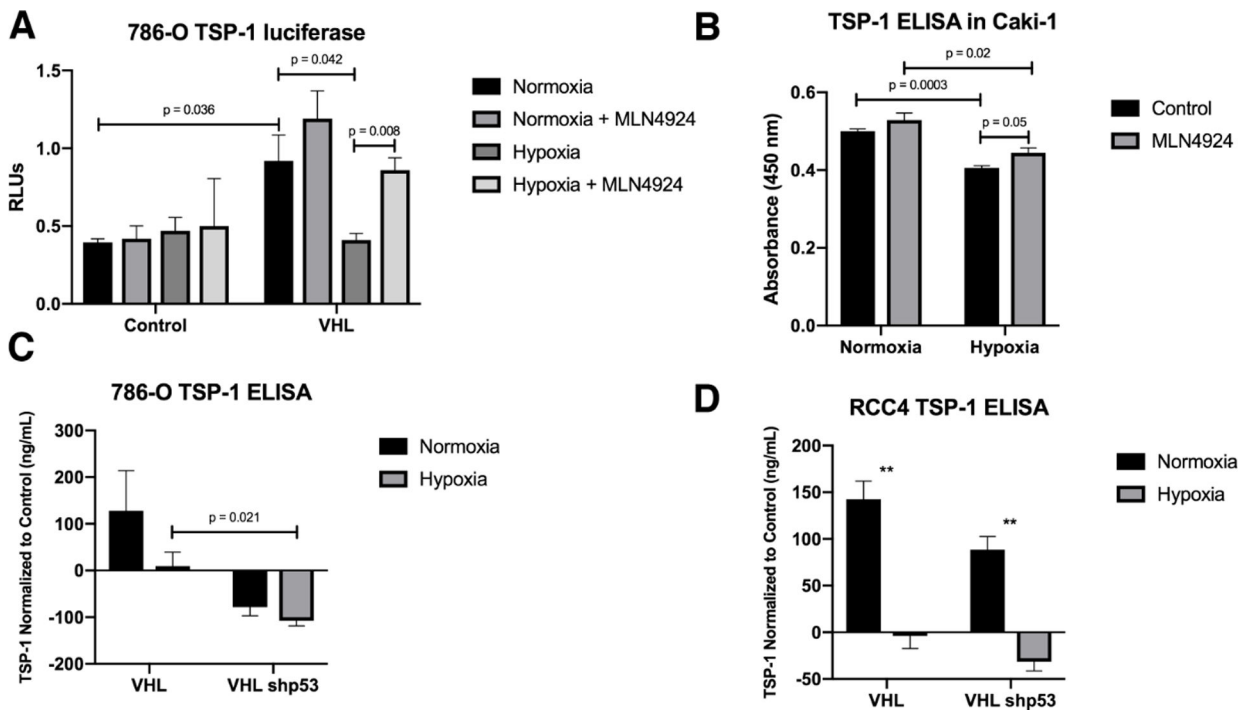


**Figure 5. VHL increases the activation of p53 under hypoxia leading to increased transcription and secretion of TSP-1**

(A) Luciferase assay for thrombospondin-1 in 786-O cells treated with MLN4924 and subjected to hypoxia. Means are plotted as relative luciferase units and calculated from three biological replicates. Error bars represent SEM. Statistics were calculated using an unpaired t test.

(B) Enzyme-linked immunosorbent assay for TSP-1 using a 10% dilution of conditioned media from Caki-1 cells treated with MLN4924 under hypoxia. Means from three biological replicates are plotted. Error bars represent SEM. Statistics were calculated using an unpaired t test.

(C-D) Enzyme-linked immunosorbent assay for TSP-1 using a 10% dilution of conditioned media from 786-O (C) or RCC4 (D) cells with knockdown p53 under hypoxia. Means from three biological replicates are plotted. Error bars represent SEM. Statistics were calculated using an unpaired t test (\* $p < 0.05$ , \*\* $p < 0.01$ , \*\*\* $p < 0.001$ ).

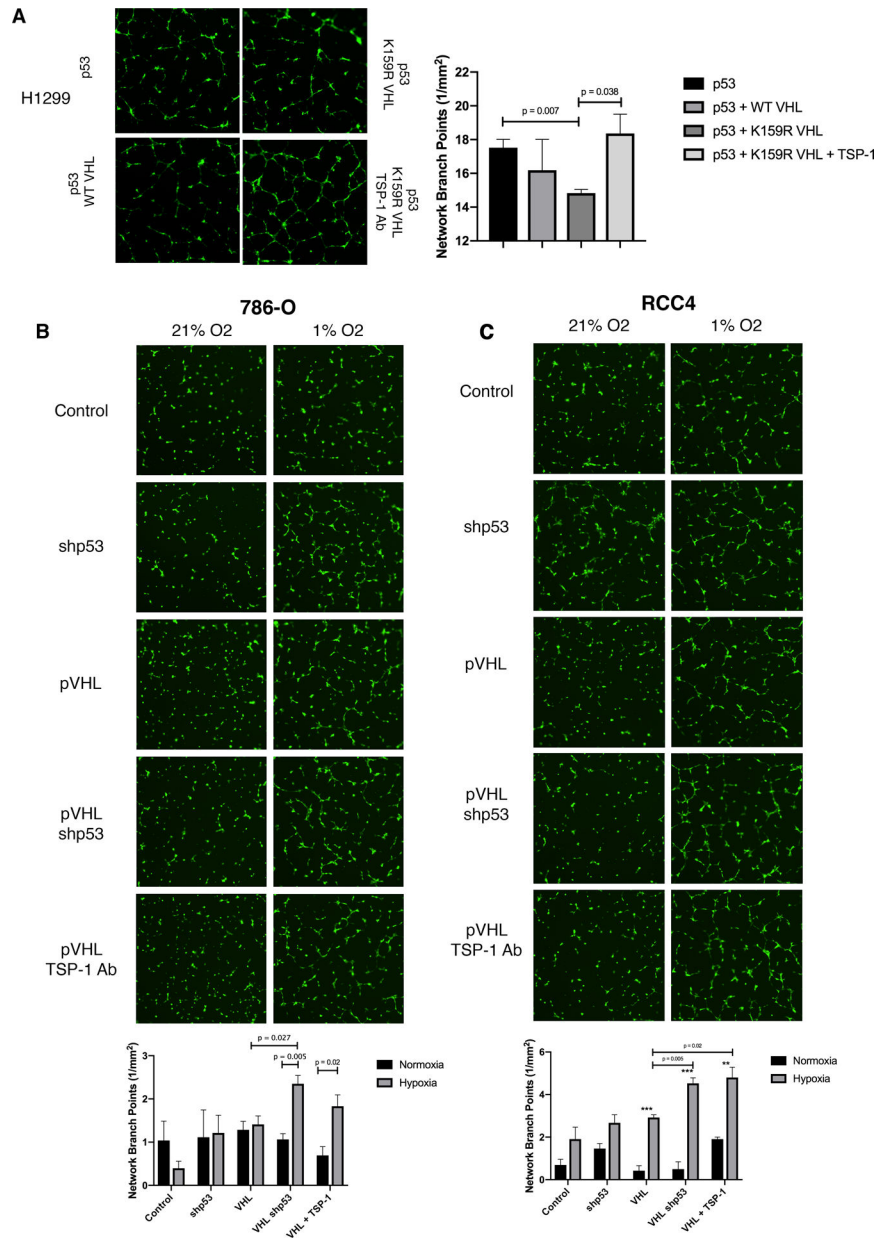


**Figure 6. p53 and TSP-1 inhibit Human Umbilical Vein Endothelial Cell network formation**  
 (A) Network formation assay using conditioned media from transiently transfected H1299 cells. Network branch points were quantified and plotted as the mean of three biological replicates. Error bars represent SEM. Statistics were calculated with an unpaired t test.  
 (B-C) Network formation assay using conditioned media from 786-O (B) or RCC4 (C) cells with VHL, VHL with knockdown p53, or VHL and an antibody against TSP-1 under normoxia or hypoxia. Network branch points were quantified and plotted as the mean of three biological replicates. Error bars represent SEM. Statistics were calculated with an unpaired t test (\* $p < 0.05$ , \*\* $p < 0.01$ , \*\*\* $p < 0.001$ ).